# High Throughput Screening and Molecular Docking Analysis on DNA Polymerase (Pol) B Cancer Variant K289M

**Nitanshu Kumar[1], Uma Kumari[2], Mahiya Noor[3], Anurag Tripathi[4]**

[1]*Trainee at Bioinformatics Project and Research Institute, Noida, India*
[2]*Senior Bioinformatics Scientist, Bioinformatics Project and Research Institute, Noida - 201301, India. Email: uma27910@gmail.com*
[3]*Trainee at Bioinformatics Project and Research Institute, Noida, India*
[4]*Trainee at Bioinformatics Project and Research Institute, Noida, Noida, India*
*Corresponding Author: Uma Kumari*

**KEYWORDS**
DNA polymerase β; K289M mutation; cancer; molecular docking; high-throughput screening; CB Dock; SwissDock; PyMOL; PDBSum; protease inhibitors.

**ABSTRACT**
DNA polymerase (pol) β plays a critical role in DNA repair mechanisms, and mutations in this enzyme have been implicated in various cancers. Because it may play a role in oncogenesis by altering the fidelity of DNA synthesis, the K289M variation of pol β is particularly interesting. This study uses Python molecular graphic, Cavity based docking, SwissDock, Structure validation server among other computational tools to undertake high-throughput screening and molecular docking investigations of DNA pol β cancer variant K289M (PDB ID: 6NKR). Ligands such as Boceprevir, Nirmatrelvir, Ritonavir, Carmofur, and Lopinavir were docked to identify potential inhibitors targeting this variant. Structural validation using the SAVES server and topology analysis using PDBSum helped assess the quality of the protein structure. Our results highlight several binding pockets with strong ligand affinities, suggesting potential therapeutic interventions for targeting pol β K289M in cancer.

## 1. Introduction

DNA polymerase β (pol β) is a crucial enzyme involved in the BER (base excision repair) pathway, which is responsible for repairing damaged or mispaired bases in the DNA through single-strand break repair mechanisms. As such, pol β plays an essential role in maintaining genome integrity. If this repair pathway is weakened, it may result in mutations that eventually mount up and cause genomic instability as well as perhaps cancer. It has been discovered that mutations in pol β affect the enzyme's fidelity, activity, and interactions with other proteins or nucleotides, which in turn affects how well DNA repair works. The K289M variation is one example of such a mutation, where methionine (M) is substituted for lysine (K) at position 289. Because it decreases pol β fidelity during DNA synthesis, this mutation has been linked to mutagenesis and cancer. Numerous cancers have been connected to the K289M mutation, including colorectal, lung, and breast cancers. Considering its part in the development of cancer, the K289M mutation is a desirable target for treatment. It might be able to selectively target cancer cells with weak DNA repair mechanisms or restore regular DNA repair processes by blocking its action [1, 2, 3].

Molecular docking is an established computational technique used to predict the interaction between a protein and small molecules (ligands). It allows researchers to model the binding of potential inhibitors to the active or allosteric sites of proteins. In this study, we employed high-throughput docking approaches using CB Dock and SwissDock to assess the interaction of the K289M variant of DNA pol β proteomic sample with several small molecule inhibitors. The ligands selected for docking—Boceprevir, Nirmatrelvir, Ritonavir, Carmofur, and Lopinavir—are known protease inhibitors that have demonstrated therapeutic potential in other disease contexts, such as viral infections (e.g., Hepatitis C and HIV) [4, 5, 6, 7, 8]. We postulated that these ligands could bind to pol β K289M and perhaps decrease its oncogenic activity, given their binding capabilities. To verify the integrity of the protein structure under study, structural validation is crucial in addition to docking experiments.

## 2. Materials and Methods

The 3D structure of DNA polymerase β K289M (PDB ID: 6NKR) was retrieved from the Protein Data Bank. Ligands selected for docking studies were Boceprevir (PubChem ID: 10324367), Nirmatrelvir (PubChem ID: 155903259), Ritonavir (PubChem ID: 392622), Carmofur (PubChem ID: 2577), and Lopinavir (PubChem ID: 92727). These ligands are established protease inhibitors that were selected based on their therapeutic potential and ability to bind to various target proteins in previous studies. Each ligand was downloaded from PubChem

[9, 10]. Molecular docking studies were carried out using two different platforms—CB Dock and SwissDock—to provide a comparative analysis of the ligand binding affinities. For CB Dock, the protein structure was uploaded, and the server automatically identified potential binding pockets(18.19,21). Each ligand was then docked into the predicted binding sites to evaluate binding affinities based on the Vina score, a measure of the predicted free energy of binding. The best binding poses were selected for further analysis. Similarly, SwissDock was used to predict the most favorable binding interactions between the protein and ligands. SwissDock ranks binding poses based on energy minimization and provides an AC score, representing the approximate free energy of the protein-ligand complex. SwissParam scores were also calculated to evaluate the drug-likeness and interaction stability of each ligand [11, 12, 13]. The 6NKR protein structure was validated using the SAVES server, which applied the VERIFY tool to assess the overall quality of the protein model. The VERIFY tool compares the observed 3D conformation of the protein with expected geometrical standards based on a dataset of known structures [14]. The protein's structural integrity was evaluated using the raw and averaged scores from the validation results, which were displayed in a graph. Using PDBSum, secondary structure and topological analysis were carried out in addition to structural validation. The alpha-helices, beta-strands, and loops that make up the protein's secondary structure are described in depth by PDBSum. The protein's helices and linking loops were shown graphically in the topology diagram, which shed light on the structural makeup of the 6NKR variation [15]. Ligand-protein interactions were visualized using PyMOL, where docking results were imported, and binding poses were analyzed. Critical residues within the binding pockets were identified, and the nature of the interactions (e.g., hydrophobic interactions, hydrogen bonding) was assessed [16].

## 3. Result and Discussion

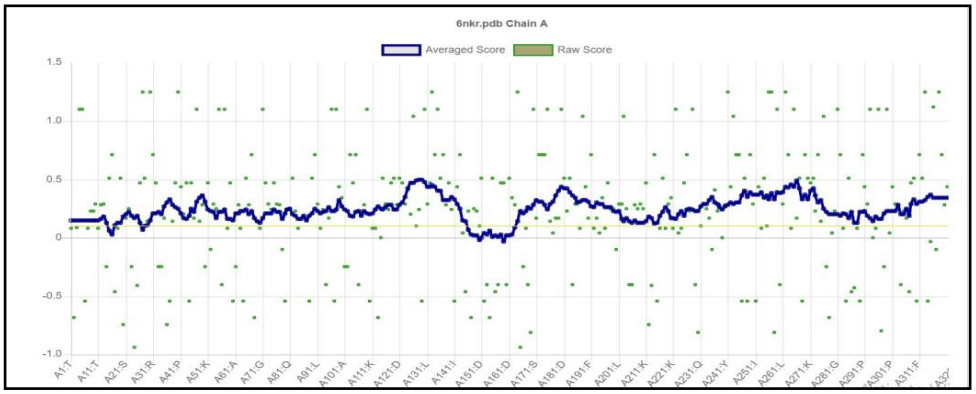


Figure 1: Graph to show quality of 3D structure of protein obtained through SAVES server's VERIFY tool

The graph depicts the VERIFY analysis results for the 6nkr Chain A, obtained from the SAVES server. In this graph, raw scores (green dots) and averaged scores (blue line) are plotted along the amino acid sequence of the protein. The raw ratings show great variance in the quality of local structural regions, with some points falling below 0.0 and others attaining values near to 1.0. Well-modeled regions are indicated by values close to or above 1.0, whilst poorly modeled areas or structural anomalies may be indicated by values below 0.0. The averaged score smooths out these fluctuations, revealing that most of the structure has an averaged score around 0.5, which suggests that the protein generally conforms to expected geometric standards. There are dips and peaks in the averaged score, notably between residues A141 and D161, where the averaged score drops below 0.0. This points to an area that might have structural problems or deviates from the geometry as it should. Overall, the VERIFY study indicates that 6nkr Chain A has high structural quality.

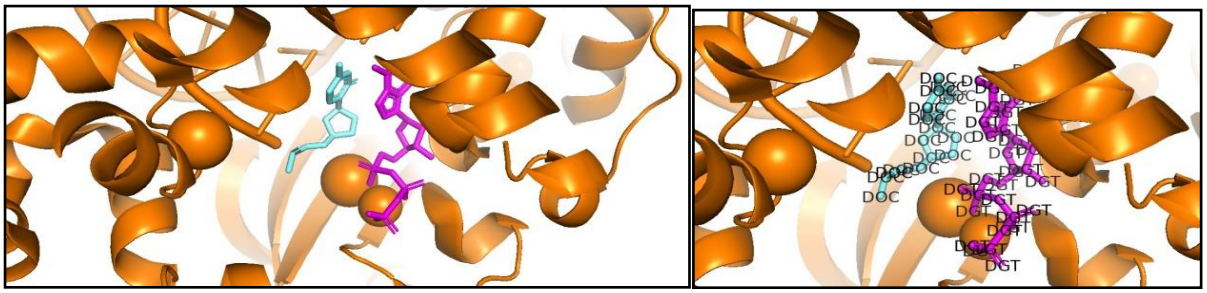

Figure 2: Ligand visualization on 6nkr with PyMol

Important interactions between the 6nkr protein and its ligands have been shown by the PyMOL visualization of the protein. With the help of important residues, the ligands are firmly positioned inside the protein's hydrophobic nooks. This provides insight into how the ligands are likely to influence the protein's function or structure, and these interactions can be further explored for therapeutic design.

- Ligand 1 (Cyan): Appears to fit within a hydrophobic pocket created by surrounding residues, forming critical interactions.
- Ligand 2 (Magenta): Seems to be engaging in potential π-π interactions or hydrogen bonding with aromatic residues and other polar residues in the protein.

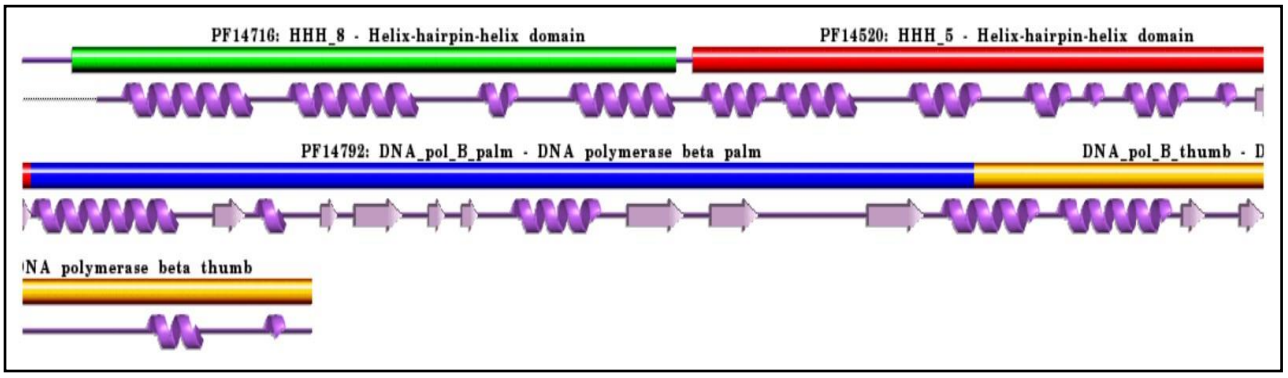


Figure 3: Secondary structure analysis obtained using PDBSum

The HHH_8 Helix-hairpin-helix domain, also referred to as the PF14716 domain, has a classical motif that is essential for DNA binding. Another Helix-hairpin-helix domain, PF14520, suggests the existence of an additional possible nucleic acid or DNA binding surface. The DNA polymerase beta palm is represented by the PF14792 domain, which constitutes the catalytic core of the enzyme. Two essential activities of the enzyme are DNA binding and nucleotide polymerization, which are carried out by this domain. The beta-strands, which are shown as arrow-shaped characteristics, and the alpha-helices, which are represented by purple helical structures, show how the secondary structure elements are arranged overall in the protein. This configuration sheds information on the functional domains of the protein by showing how the various structural components are arranged to facilitate the enzyme's involvement in DNA synthesis and repair.

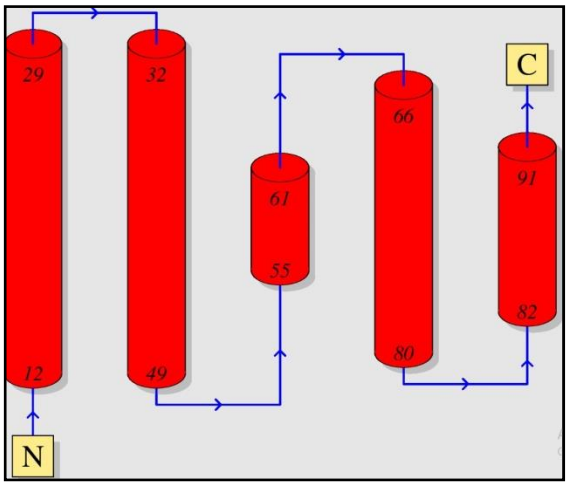


Figure 4: Protein topology obtained using PDBSum

The topology diagram of the protein shows the arrangement of alpha-helices (red cylinders) and their connections through loops (blue lines). These secondary structures are situated at residue locations 12, 29, 32, 49, 55, 61, 66, 80, 82, and 91, as indicated by the sequential numbering of the helices. The diagram shows the general flow and structural connection of the helices within the protein, starting at the N-terminal (labeled N) and ending at the C-terminal (labeled C). Unstructured areas, or loops, are represented by the blue lines that connect the helices and aid in the folding and structural arrangement of the protein. This visualization provides insights into the protein's possible functional areas or contact locations by making it easier to see how the alpha-

helices are grouped and how the protein folds into its three-dimensional structure.

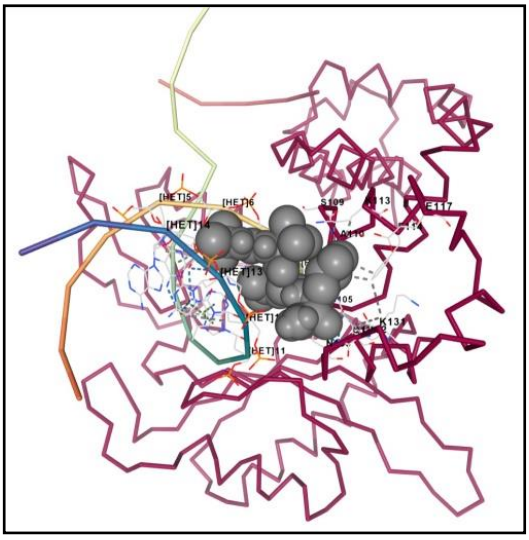

Figure 5: Docking image with Boceprevir through CBDock (pubchem id-10324367)

**Table 1: Docking image with Boceprevir through CBDock**

| CurPocket ID | Vina Score | Cavity Volume (Å³) | Center (x, y, z) | Docking Size (x, y, z) |
|---|---|---|---|---|
| C2 | -9.7 | 993 | 14, 20, 21 | 23, 23, 23 |
| C5 | -8.7 | 173 | 6, 12, 14 | 23, 23, 23 |
| C3 | -8.0 | 336 | 19, 8, 18 | 23, 23, 23 |
| C1 | -8.2 | 1223 | 12, 4, 4 | 23, 23, 23 |
| C4 | -7.4 | 217 | 22, -2, -23 | 23, 23, 23 |

These results indicate the protein-ligand interactions with their respective binding scores (Vina score), and the pocket C2 shows the best binding affinity with a score of -9.7. The interacting residues within Pocket C2 from Chain A are:

GLY105, SER109, ALA110, LYS113, PHE114, GLU117, ASP130, LYS131, LEU132, ASN133, GLN136, LYS230, GLY231, GLU232. The interacting residues (e.g., GLY105, SER109, PHE114, LYS230) form a part of the protein-ligand interface, which is essential for stabilizing the ligand within the pocket. These residues may participate in hydrogen bonding (e.g., through polar residues like SER109, ASP130, ASN133) or hydrophobic interactions (e.g., through nonpolar residues like ALA110, LEU132).

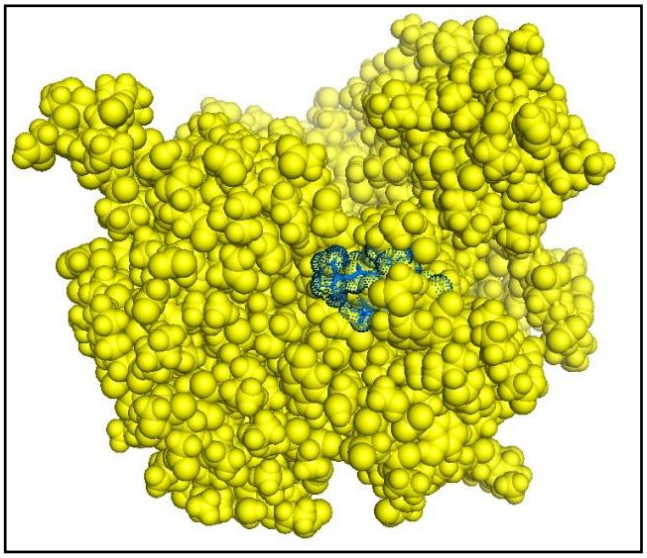

Figure 6: Docking image with Boceprevir through SwissDock (pubchem id-10324367)

The docking study conducted using SwissDock generated clusters with their respective AC scores (Approximate Free Energy) and SwissParam scores.

**Table 2: Docking image with Boceprevir through SwissDock**

| Cluster Number | Cluster Member | AC Score | SwissParam Score |
|---|---|---|---|
| 0 | 1 | 246.527274 | -8.2932 |
| 1 | 1 | 249.396677 | -8.4083 |
| 2 | 1 | 250.114173 | -8.6940 |
| 3 | 1 | 253.974933 | -8.1104 |
| 4 | 1 | 254.696738 | -8.0393 |
| 5 | 1 | 254.837325 | -7.5685 |

The best binding cluster (Cluster Number: 0) had an AC score of 246.527274 and a SwissParam score of -8.2932, indicating a favorable binding interaction. Cluster 2 showed the highest SwissParam score of -8.6940, suggesting that this cluster had the strongest binding interaction according to SwissDock. Overall, SwissDock demonstrated multiple favorable clusters, with SwissParam scores between -7.5685 and -8.6940, indicating strong binding interactions across the top clusters. Boceprevir is a potent protease inhibitor initially developed for the treatment of Hepatitis C. To explore its binding interactions and affinity with the given target protein, a docking study was conducted using two different docking platforms, CB-Dock and SwissDock. The structural insights and binding energies were evaluated to determine the best binding pose and affinity of Boceprevir to the 6nkr.

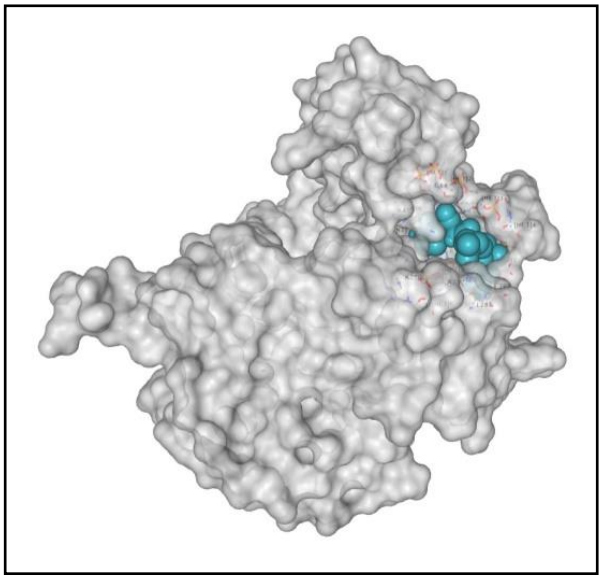

Figure 7: Docking image with Nirmatrelvir through CBDock (pubchem id-155903259)

**Table 3: Docking image with Nirmatrelvir through CBDock**

| CurPocket ID | Vina Score | Cavity Volume (Å³) | Center (x, y, z) | Docking Size (x, y, z) |
|---|---|---|---|---|
| C1 | -9.0 | 1233 | 12, 4, 4 | 22, 22, 22 |
| C5 | -9.0 | 173 | 6, 12, 14 | 22, 22, 22 |
| C2 | -8.6 | 993 | 14, 20, 21 | 22, 22, 22 |
| C3 | -8.2 | 336 | 19, 8, 18 | 22, 22, 22 |
| C4 | -6.9 | 217 | 22, -2, -23 | 22, 22, 22 |

The best binding pocket (CurPocket ID: C1) had a Vina score of -9.0, representing the most favorable interaction. Pocket C5 also had a Vina score of -9.0, but a much smaller cavity volume of 173 Å³, indicating that Pocket C1 is the most spacious and favorable for ligand binding. The remaining pockets (C2-C4) showed lower Vina scores, suggesting less favorable binding affinity compared to C1 and C5. Interacting Residues of Pocket C1: HIS34, ASN37, ALA38, LYS41, PRO63, GLY64, LYS280, ASN281, MET282, ALA284, HIS285, LEU287, GLU288, TRP325, GLU335

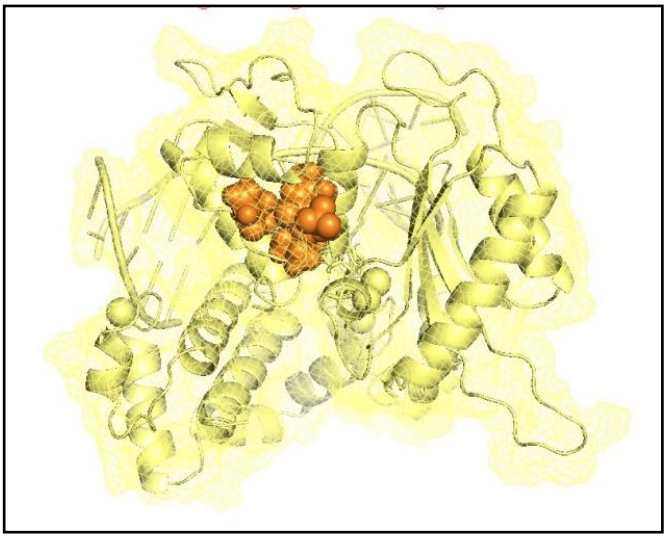

Figure 8: Docking image with Nirmatrelvir through SwissDock (pubchem id-155903259)

**Table 4: Docking image with Nirmatrelvir through SwissDock**

| Cluster Number | Cluster Member | AC Score | SwissParam Score |
|---|---|---|---|
| 0 | 1 | -89.932462 | -9.6694 |
| 1 | 1 | -85.484405 | -10.4443 |
| 2 | 1 | -84.644679 | -9.3706 |
| 3 | 1 | -84.307850 | -9.2251 |
| 4 | 1 | -83.850857 | -10.3462 |
| 5 | 1 | -83.681843 | -9.4887 |

The best cluster (Cluster 1) exhibited a SwissParam score of -10.4443, indicating a strong binding affinity. Cluster 0 had a SwissParam score of -9.6694, but a slightly better AC score than Cluster 1. The top 10 clusters show moderate to strong binding affinities, with SwissParam scores ranging from -6.9411 to -8.4081, suggesting stable interactions of Nirmatrelvir with the target protein.

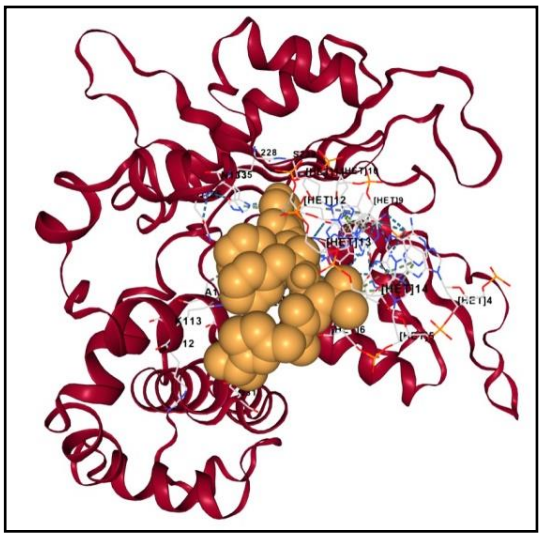

Figure 9: Docking image with Ritonavir through CBDock (pubchem id-392622)

**Table 5: Docking image with Ritonavir through CBDock**

| CurPocket ID | Vina Score | Cavity Volume (Å³) | Center (x, y, z) | Docking Size (x, y, z) |
|---|---|---|---|---|
| C2 | -9.7 | 993 | 14, 20, 21 | 29, 29, 29 |
| C1 | -9.5 | 1223 | 12, 4, 4 | 29, 29, 29 |
| C3 | -9.1 | 336 | 19, 8, 18 | 29, 29, 29 |
| C5 | -8.3 | 173 | 6, 12, 14 | 29, 29, 29 |
| C4 | -6.9 | 217 | 22, -2, -23 | 29, 29, 29 |

Ritonavir, a protease inhibitor commonly used in the treatment of HIV, has been explored for its potential

interactions with the target protein using two docking tools: CB-Dock and SwissDock. Pocket C2 showed the strongest binding affinity with a Vina score of -9.7, a large cavity volume of 993 Å³, and pocket center coordinates at (14, 20, 21). This suggests that C2 is the most favorable binding site for Ritonavir. Interacting Residues in Pocket C2: Lys27, Gln31, Ala32, Ile33, His34, Tyr36, Asn37, Gly105, Pro108, Ser109, Ala110, Arg112, Lys113, Phe114, Glu117, Lys131, Leu132, Asn133, His135, Gln136, Leu228, Ser229, Met236.

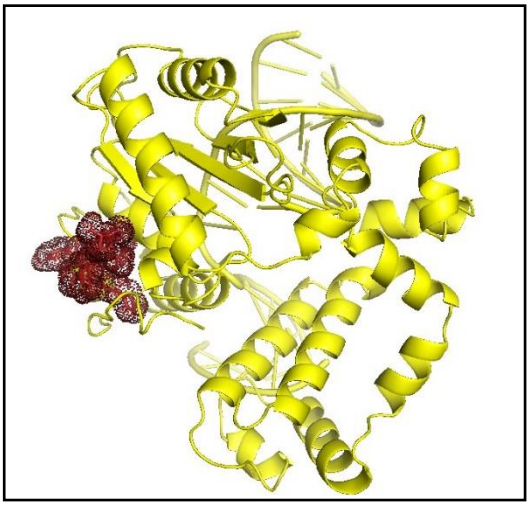

Figure 10: Docking image with Ritonavir through SwissDock (pubchem id-392622)

**Table 6: Docking image with Ritonavir through SwissDock**

| Cluster Number | Cluster Member | AC Score | SwissParam Score |
|---|---|---|---|
| 0 | 1 | -89.932462 | -9.6694 |
| 1 | 1 | -85.484405 | -10.4443 |
| 2 | 1 | -84.644679 | -9.3706 |
| 3 | 1 | -84.307850 | -9.2251 |
| 4 | 1 | -83.850857 | -10.3462 |
| 5 | 1 | -83.681843 | -9.4887 |

Cluster 0 showed the most favorable binding pose, with an AC score of -89.932462 and a SwissParam score of -9.6694. Cluster 1 exhibited an even stronger SwissParam score of -10.4443, suggesting a highly stable interaction. Ritonavir exhibits strong binding potential to the target protein, with Pocket C2 identified by CB-Dock as the most favorable binding site (Vina score: -9.7) and Cluster 0 identified by SwissDock showing the most favorable docking pose (AC score: -89.932462). The identified interacting residues within Pocket C2 suggest robust hydrophobic and hydrogen bonding interactions that could be further explored for therapeutic implications.

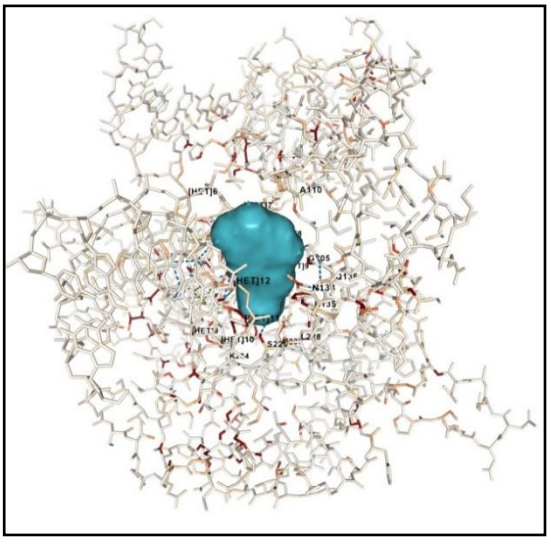

Figure 11: Docking image with Carmofur through CBDock (pubchem id-2577)

**Table 7: Docking image with Carmofur through CBDock**

| CurPocket ID | Vina Score | Cavity Volume (Å³) | Center (x, y, z) | Docking Size (x, y, z) |
|---|---|---|---|---|
| C2 | -7.4 | 993 | 14, 20, 21 | 21, 21, 21 |
| C1 | -6.2 | 1223 | 12, 4, 4 | 21, 21, 21 |
| C5 | -6.2 | 173 | 6, 12, 14 | 21, 21, 21 |
| C3 | -6.1 | 336 | 19, 8, 18 | 21, 21, 21 |
| C4 | -5.5 | 217 | 22, -2, -23 | 21, 21, 21 |

Pocket C2 displayed the highest binding affinity, with a Vina score of -7.4 and a cavity volume of 993 Å³. Interacting Residues in Pocket C2: GLY105, ILE106, SER109, ALA110, PHE114, LYS131, ASN133, HIS135, GLN136, LEU228, SER229, LYS234, MET236. Pocket C1 exhibited a larger cavity volume of 1223 Å³, though its Vina score was lower at -6.2. The remaining pockets (C3, C4, and C5) demonstrated weaker binding interactions with Vina scores ranging from -5.5 to -6.2.

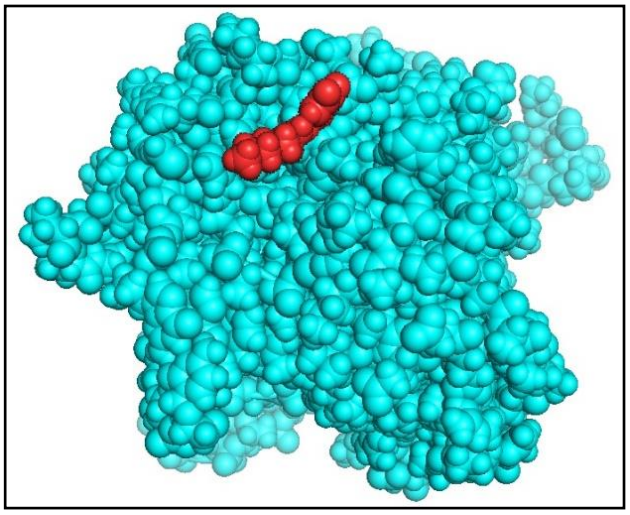

Figure 12: Docking image with Carmofur through SwissDock (pubchem id-2577)

Table 8: Docking image with Carmofur through SwissDock

| Cluster Number | Cluster Member | AC Score | SwissParam Score |
|---|---|---|---|
| 0 | 1 | -114.594927 | -7.7958 |
| 1 | 1 | -112.735532 | -7.5258 |
| 2 | 1 | -112.217684 | -7.6138 |
| 3 | 1 | -112.071264 | -7.3020 |
| 4 | 1 | -111.714004 | -7.4586 |
| 5 | 1 | -110.699404 | -7.2212 |

Cluster 0 exhibited the most favorable docking pose, with an AC score of -114.594927 and a SwissParam score of -7.7958, indicating a stable binding interaction. Carmofur exhibited favorable binding to the target protein, with Pocket C2 identified by CB-Dock as the most promising site (Vina score: -7.4). SwissDock results further confirmed this, identifying Cluster 0 as the best binding pose (AC score: -114.594927). The interacting residues from both platforms suggest a combination of hydrophobic interactions and hydrogen bonding, which stabilize Carmofur's binding to the protein.

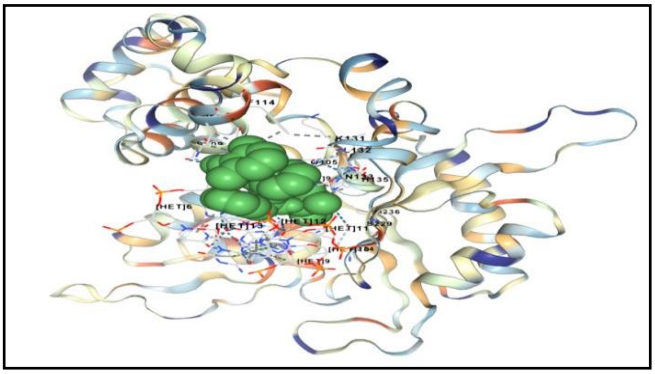

Figure 13: Docking image with Lopinavir through CBDock (pubchem id-92727)

**Table 9: Docking image with Lopinavir through CBDock**

| CurPocket ID | Vina Score | Cavity Volume (Å³) | Center (x, y, z) | Docking Size (x, y, z) |
|---|---|---|---|---|
| C2 | -9.6 | 993 | 14, 20, 21 | 24, 24, 24 |
| C5 | -9.2 | 173 | 6, 12, 14 | 24, 24, 24 |
| C3 | -8.9 | 336 | 19, 8, 18 | 24, 24, 24 |
| C1 | -8.8 | 1223 | 12, 4, 4 | 24, 24, 24 |
| C4 | -7.0 | 217 | 22, -2, -23 | 24, 24, 24 |

Pocket C2 exhibited the best binding affinity with a Vina score of -9.6 and a cavity volume of 993 Å³, making it the most favorable binding site for Lopinavir. Interacting Residues in Pocket C2: GLY105, ILE106, GLY107, SER109, ALA110, LYS113, PHE114, GLU117, LYS131, LEU132, ASN133, HIS135, GLN136, SER229, LYS234, MET236.

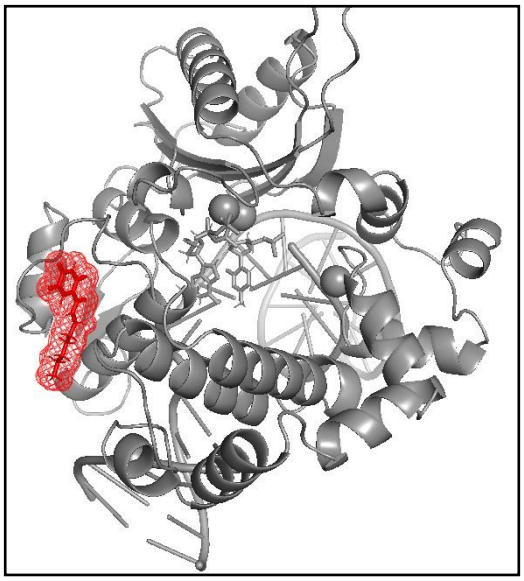

Figure 14: Docking image with Lopinavir through SwissDock (pubchem id-92727)

**Table 10: Docking image with Lopinavir through SwissDock**

| Cluster Number | Cluster Member | AC Score | SwissParam Score |
|---|---|---|---|
| 0 | 1 | 303.246689 | -7.8907 |
| 1 | 1 | 305.097410 | -8.4081 |
| 2 | 1 | 306.197537 | -7.7284 |
| 3 | 1 | 307.383100 | -7.9376 |
| 4 | 1 | 308.514592 | -7.6587 |
| 5 | 1 | 309.285081 | -6.9411 |

Lopinavir showed strong binding interactions with the target protein, particularly in Pocket C2 identified by CB-Dock (Vina score: -9.6). SwissDock further confirmed the binding stability, with Cluster 1 having the most favorable SwissParam score (-8.4081). Lopinavir, a protease inhibitor used in HIV treatment, has been analyzed for its binding interactions with the target protein using CB-Dock and SwissDock.

## 4. Conclusion

In this study, we performed high-throughput molecular docking and structural analysis of the DNA polymerase β cancer variant K289M to identify potential therapeutic inhibitors. Our results revealed key binding pockets with high binding affinities, particularly Pocket C2, which showed strong interactions with most ligands. Structural validation using the SAVES server confirmed the overall quality of the 6NKR structure, though some regions showed deviations from expected geometry. These results offer important information on how to target pol β K289M for cancer treatment, and more research can examine the functional ramifications of these connections to create fresh approaches to treatment.

## References

[1] Batra VK, Alnajjar KS, Sweasy JB, McKenna CE, Goodman MF, Wilson SH. Revealing an Internal Stabilization Deficiency in the DNA Polymerase β K289M Cancer Variant through the Combined Use of Chemical Biology and X-

ray Crystallography. Biochemistry. 020;59(8):955-963. doi:10.1021/acs.biochem.9b01072
[2] Lang T, Maitra M, Starcevic D, Li SX, Sweasy JB. A DNA polymerase beta mutant from colon cancer cells induces mutations. Proc Natl Acad Sci U S A. 2004;101(16):6074-6079. doi:10.1073/pnas.0308571101
[3] Alnajjar KS, Garcia-Barboza B, Negahbani A, et al. A Change in the Rate-Determining Step of Polymerization by the K289M DNA Polymerase β Cancer-Associated Variant. Biochemistry. 2017;56(15):2096-2105. doi:10.1021/acs.biochem.
[4] 6b01230
[5] Rizza SA, Talwani R, Nehra V, Temesgen Z. Boceprevir. Drugs Today (Barc). 2011;47(10):743-751. doi:10.1358/
[6] dot.2011.47.10.1656503
[7] Magro P, Zanella I, Pescarolo M, Castelli F, Quiros-Roldan E. Lopinavir/ritonavir: Repurposing an old drug for HIV infection in COVID-19 treatment. Biomed J. 2021;44(1):43-53. doi:10.1016/j.bj.2020.11.005
[8] Hammond J, Leister-Tebbe H, Gardner A, et al. Oral Nirmatrelvir for High-Risk, Nonhospitalized Adults with Covid-19. N Engl J Med. 2022;386(15):1397-1408. doi:10.1056/NEJMoa2118542
[9] Saravolatz LD, Depcinski S, Sharma M. Molnupiravir and Nirmatrelvir-Ritonavir: Oral Coronavirus Disease 2019 Antiviral Drugs. Clin Infect Dis. 2023;76(1):165-171. doi:10.1093/cid/ciac180
[10] Islam MM, Mirza SP. Versatile use of Carmofur: A comprehensive review of its chemistry and pharmacology. Drug Dev Res. 2022;83(7):1505-1518. doi:10.1002/ddr.21984
[11] Dr Uma kumari, Devanshi Gupta, In silico RNA aptamer drug design and modelling,2022/4, Journal-JETIR,Volume-9, Issue-4, Pages 718-725
[12] Tripathi, Anurag & Kumari, Uma. (2023). Comparative Analysis and Drug Target Identification of Human Kidney Cancer. International Journal for Research in Applied Science and Engineering Technology. 11. 10.22214/ijraset.2023.55777.
[13] Bugnon M, Röhrig UF, Goullieux M, Perez MAS, Daina A, Michielin O, Zoete V. SwissDock 2024: major enhancements for small-molecule docking with Attracting Cavities and AutoDock Vina. Nucleic Acids Res. 2024
[14] Röhrig UF, Goullieux M, Bugnon M, Zoete V. Attracting Cavities 2.0: improving the flexibility and robustness for small-molecule docking. J. Chem. Inf. Model., 2023
[15] Liu, Y., Yang, X., Gan, J., Chen, S., Xiao, Z. X., & Cao, Y. (2022). CB-Dock2: improved protein-ligand blind docking by integrating cavity detection, docking and homologous template fitting. Nucleic acids research, 50(W1), W159–W164. https://doi.org/10.1093/nar/gkac394
[16] Ankita Singh, Rahul Kaushik, Avinash Mishra, Asheesh Shanker, B. Jayaram, ProTSAV: A protein tertiary structure analysis and validation server, Biochimica et Biophysica Acta (BBA) - Proteins and Proteomics,Volume 1864, Issue 1,2016,Pages 11-19,ISSN 1570-9639, https://doi.org/10.1016/j.bbapap.2015.10.004.
[17] Laskowski R. A. (2001). PDBsum: summaries and analyses of PDB structures. Nucleic acids research, 29(1), 221–222. https://doi.org/10.1093/nar/29.1.221
[18] Uma Kumari, Devanshi Gupta, Study of Malignant Melonema Causing Protein “5ixb” Using Multiomics Approach, November 2022, INTERNATIONAL JOURNAL OF INNOVATIVE RESEARCH IN TECHNOLOGY , Volume 9 Issue 6 , ISSN: 2349-6002
[19] Mansi Jangir,Uma Kumari 2024,"IN-SILICO DRUG DESIGNING AND NETWORK PHARMACOLOGY ANALYSIS OF NEUROBLASTOMA BY MACHINE LEARNING", International Journal of Emerging Technologies and Innovative Research , V11, Issue 10, pp532-b542, https://doi.one/10.1729/Journal.41845
[20] Uma Kumari, Abhishek Ebenezar,etal;2024, Next Genration sequencing and Proteomics analysis of BRD2-BD1 complex with MDP5 in Medulloblastoma: COMPUTATIONAL ANALYSIS AND NGS PIPELINE FOR HUMAN GRK2 IN COMPLEX WITH G-BETA-GAMMA IN CARDIOVASCULAR DISEASE WITH BIOPYTHON,2024; Volume 6 , Issue - 14 : Page: 1993-2012 African Journal of Biological Sciences doi: 10.48047/AFJBS.6.14.2024.1992-2012
[21] Vipasha Rathi,Uma Kumari,2024 "Identification of active compound and NGS analysis BRD4-BD2 in complex with SF2523 of human malignant brain tumor", International Journal of Emerging Technologies and Innovative Research Vol.11, Issue 8,ppb597-b606, https://doi.one/10.1729/Journal.40957
[22] Uma Kumari, Unnayni Joshi, 2024 "Targeted NGS Proteomics analysis on M342R Mutation and 17+1mer Oligonucleotide with Triplet GGT", International Journal of Emerging Technologies and Innovative Research,Vol.11, Issue 6, page no. ppj785-j793, June-2024, http://doi.one/10.1729/Journal.40303
[23] Uma Kumari,Gurpreet Kaur et al,2024,”Biopython/Network Of Protein Identification And NGS Analysis Of Glioma Cancer ATP Competitive Type III C-MET Inhibitor : 7.367 (Calculated by Google Scholar) : Volume 11, Issue 2 : 27-Jun-2024 :pp 41-51 : http://doi.one/10.1729/Journal.40229